

# Influence of Linear Reciprocating and Multi-Directional Sliding on PEEK Wear Performance and Transfer Film Formation

K.A. Laux<sup>1</sup>, C.J. Schwartz<sup>2,\*</sup>

<sup>1</sup>Department of Mechanical Engineering, Texas A&M University, College Station, Texas, USA

<sup>2</sup>Department of Mechanical Engineering, Iowa State University, Ames, Iowa, USA

## Abstract

Because of their light weight, chemical resistance, and self-lubricating properties, polymers are used in applications ranging from biomedical to aerospace. Some polymers exhibit significant differences in wear resistance based on whether they are in unidirectional or multidirectional sliding. Shear induced polymer chain orientation is believed to be responsible for this behavior. Polyetheretherketone (PEEK) has excellent wear resistance, but its multidirectional sliding behavior has not been thoroughly investigated. A factorial multidirectional pin-on-plate wear study of PEEK was conducted with a focus on molecular weight and sliding path directionality. These factors were studied for their correlation to overall wear performance. Additionally, transfer film thickness was measured at locations along the wear path using white light interferometry. Wear in PEEK was shown to depend significantly on path shape and direction. The lowest wear configuration also resulted in quantifiably thinner and more continuous transfer films. A result of this work has been a greater understanding of PEEK wear mechanisms in various sliding configurations.

*Keywords:* tribology, wear, polymers, transfer film, polyetheretherketone

## 1. Introduction

Among the challenges associated with modeling wear in polymers is the fact that a small change in the polymer's molecular structure can have a profound influence on the mechanical properties. The degree of crystallinity, presence of branching, and entanglement density will all influence the viscoelastic behavior of the polymer. Unlike metals that plastically deform because of dislocation movements, polymer deformation requires chains to slide, stretch, and orient themselves in the direction of the applied stress. This reorientation phenomenon will result in strain hardening until individual chains are stretched and rupture at their ultimate stress. During wear, chain orientation has been speculated to produce significantly different results depending on sliding direction. Ultra high molecular weight polyethylene (UHMWPE) is known to demonstrate much greater wear when exposed to cross shear motion compared to unidirectional sliding [1, 2]. An early indication of this effect was because of the observation by Charnley that polymer bearing surfaces in orthopedic joints exhibited far greater wear *in vivo* than seen in laboratory unidirectional pin-on-disk wear tests [3, 4]. Wang et al. showed that a wear simulator which modeled the motion of a joint resulted in two orders of magnitude greater wear than linear reciprocating tests [1]. The vast difference in wear observed was attributed to an orientation strengthening that occurs during linear motion and an orientation softening as a result of multi-directional wear [5]. This phenomenon has been verified experimentally as well as theoretically. Scanning electron microscope (SEM) inspection of the plasma etched wear surface of UHMWPE has shown that the surface is stretched and crystal structure becomes oriented anisotropically [5]. Wang et al. proposed that this structural anisotropy promotes rupture between oriented chains. It was suggested and later proven [6] that low wear could be achieved by preventing this molecular reorganization through irradiation crosslinking [7]. Sambasivan showed that UHMWPE chains align parallel to the sliding direction by measuring the X-ray absorption spectra of the worn pin surface. Wear was believed to result from fracture of the unaligned

\* Corresponding author at: email: cris1@iastate.edu; phone: 1-515-294-2866

loose chains [8]. When the strain energy effects of softening and orientation are accounted for, wear models have been able to accurately predict wear as a function of cross shear [9]. Irrespective of the underlying molecular dynamics, advances in UHMWPE bearing surfaces of implanted artificial joints have been made from knowledge of chain orientation during wear. However, techniques applied to UHMWPE to restrict chain orientation and improve wear performance may not be practical or possible in all polymers.

The molecular structure of polymers and its effect on friction and wear was first studied by Pooley and Tabor [10]. The low friction (COF <0.1) and material transfer behavior of polyethylene (PE) and polytetrafluoroethylene (PTFE) are a result of a smooth molecular profile and is independent of the crystallinity. The introduction of bulky side groups was shown to affect this behavior and it was believed the side groups prevented chains from orienting themselves into a smooth surface [10]. Poly(ether-etherketone) or PEEK is an aromatic-backbone semicrystalline polymer belonging to the polyaryletherketone (PAEK) family of thermoplastics. In wear applications, friction is relatively high (COF ~0.3) but the polymer is capable of forming a protective tribofilm. Unlike polytetrafluoroethylene (PTFE) that forms a film due to its layered lamellae structure [11], the exact mechanism for PEEK transfer films is unknown. The formation of a transfer film is regarded to be integral in PEEK wear resistance. The film's rheological behavior, cohesiveness, and adherence to the substrate will all determine how effectively it can protect the bulk polymer from wear [12]. Surface roughness has been found to be a governing factor in PEEK wear and its relation to transfer film has been widely studied. Ovaert investigated the effects of counterface roughness on PEEK and found a minimum in wear occurred at roughness of  $0.15\mu\text{m R}_Q$  [13]. At roughness below this, debris morphology changes indicating a difference in wear mechanism. Wear in polymers can generally be categorized in terms of adhesive, abrasive, and fatigue wear [14]. Adhesive wear implies that the polymer becomes bound to the underlying substrate and debris is generated during the shearing of the junction. Abrasive and fatigue wear however depend on hard asperities removing material from the softer bulk polymer through plowing and subsurface cracking, respectively. In theory, development of a transfer film will protect the polymer from wear by covering sharp surface features. Additionally, since the film's modulus better matches the bulk polymer, subsurface stresses will also be reduced. Despite the general acceptance that transfer films are key in reducing PEEK wear, no clear understanding of an underlying mechanism for their formation exists. In polymer wear, it is believed that film formation is

when the counterface is excessively smooth, wear in polymers is accelerated since there is a lack of transfer film generating surface features [15]. PEEK wear has also been observed to depend on the sliding direction relative to the surface roughness direction. Friedrich et al. observed wear to be more sensitive to increases in surface roughness when sliding was parallel to the roughness orientation and attributed it to a lack of transfer film formation [16]. Similarly, Ovaert observed the inability of PEEK to form continuous transfer films when surface roughness was angled relative to the sliding direction [17]. However, the vast majority of wear investigation of PEEK as it relates to transfer film generation has employed a pin-on-disk configuration where only unidirectional sliding is studied.

In this study, two grades of PEEK that differed in molecular weight were investigated using various sliding path shapes and directionalities to determine a relationship between wear and sliding orientation. A pin-on-plate tribometer was built that is capable of producing both linear and circular reciprocating paths. The experiment was designed so that sliding speed, distance, and calculated contact pressure were duplicated for circular and linear wear paths. In addition to wear, metrics were developed to objectively characterize and compare transfer film thickness and continuity between tests in order to help explain how PEEK wear is dependent on transfer film formation.

## **2. Materials and Methods**

## 2.1 Materials

Samples from two different grades of PEEK material from the same supplier were used in this experiment. Identity of the supplier and grades has been withheld due to contractual obligations to the sponsor of the work; however, mechanical and morphological properties of the materials were measured and are reported below. Samples were injection molded and finish machined into various geometry test specimens. The details of the molding process are as follows: All specimens were machined from tubular stock shapes with an outer diameter of 152 mm and inner diameter of 127 mm on an injection molding press (Cincinnati), with an oil heated mold and base and an 80-mm low shear profile screw. The pelletized materials were dried in a forced-air, electrically-heated commercial dryer system containing a desiccant pack before molding to attain a weight percent moisture of less than 0.015% as measured by a moisture analyzer (Sartorius LMA100P). The temperature profile in the screw, conveying and nozzle sections of the injection molder were: a 377°C set point for the rear, center and front zone temperature controllers; a 371°C set point for the adapter and nozzle; and a 404°C set point for the hot sprue. This profile resulted in a melt temperature at the nozzle of 394°C. The mold temperature for the mold surface defining the inside diameter of the tube was set to 204°C, with the outer diameter mold surface set to 193°C, with a cooling time of 250 s in the mold post injection and final packing. Residence time of the resin in the barrel of the molding machine was approximately 360 s.

The materials are graded according to their viscosity, which correlates directly to molecular weight  $M_w$ . Therefore, the selected grades ‘L’ and ‘H’ represent samples of low and high molecular weight, respectively. Gel permeation chromatography (GPC) was used to measure molecular weight and polydispersity index (PDI), and the results are shown in Table 2. Additionally, the degree of crystallinity was found through differential scanning calorimetry (DSC) and viscoelastic properties were found using dynamic mechanical analysis (DMA). These properties are also reported in the table.

**Table 1.** Compilation of morphological (weight average molecular weight,  $M_w$ , and polydispersity index, PDI, and crystallinity) and viscoelastic data (storage and loss moduli) for the two PEEK grades used in the study.

Sample	$M_w$	PDI	% crystallinity	Storage Modulus (GPa)	Loss Modulus (MPa)
L	66200	2.62	48	3.41	60.5
H	114362	3.11	42	3.11	69.4

## 2.2 Wear Testing

Volumetric wear was measured by determining the volume of material lost during wear testing. For this work, a tribometer with two axes of motion was constructed using two programmable linear stages (Aerotech). The tribometer allows for sliding of pin specimens against planar counterfaces under an applied normal load along a specified wear path and sliding velocity. The stages each move independently and the combined motion of each stage determines the programmed wear path and velocity. The wear pins themselves remain stationary and are loaded against the counterfaces using pneumatically controlled actuators. Counterfaces were surface ground so the roughness was oriented in a single direction. This means that a circular path would result in a continuously changing orientation of surface roughness relative to the pin direction of motion. The goal of this experiment was to determine if wear path shape has a significant effect on wear in PEEK. With all other parameters fixed, a difference in wear would indicate that a multi-directional wear path influences PEEK differently than unidirectional motion. Additionally, it was desired to know if reciprocating motion will result in different wear behavior than an overlapping motion. To investigate this, four different wear paths, shown in Figure 9, were programmed so that an average velocity of 0.2 m/s was achieved. The total wear path distance of 2 km for an individual pin was the same for all four paths. These paths were selected so the influence of both multidirectional motion and reciprocating motion could be studied. Circular configurations were

programmed to have a radius of 10 mm and were run for 32,000 cycles (approx. 2km sliding distance) in order to ensure steady state wear was reached. However, the circular paths studied differed in their velocity profile and/or directionality. A constant velocity circular (CVC) path involved a constant 0.2 m/s. However, in order to produce a reciprocating circular (RC) path, motion had to come to a complete stop and accelerate after each pass. The acceleration after each stop was set to  $3 \text{ m/s}^2$  in order to achieve an average velocity of 0.2 m/s for the test. Accounting for the time and distance required for acceleration from zero (and return to zero at the end of the cycle), this resulted in a maximum (fixed) velocity of 0.27 m/s over approximately 90% of the wear path distance. Similarly, a variable velocity circular (VVC) test configuration was used that also accelerated at  $3 \text{ m/s}^2$ ; however, motion overlapped in the same direction after each pass rather than reciprocate. In order to study the effect of uni-directional sliding, a linear reciprocating (LR) motion was used. Although the shape profile differed from the circular tests, acceleration and average velocity were identical to the (VVC) and (RC) tests. For the circular wear path, the angle between the direction of the pin motion and the counterface roughness direction was constantly changing. The linear reciprocating motion was set at an angle of 45 degrees relative to the counterface roughness direction. Thus, over the entire wear circuit, the wear pin was exposed to the same average surface roughness despite differences in wear path.

Testing was conducted using applied loads of 34 N (low) and 160 N (high), which resulted in Hertzian calculated pressures of 1.1 MPa and 5.1 MPa, respectively. Hardened D2 tool steel counterface plates (HRC 56.6 measured) were ground so that roughness was oriented in one direction with a measured roughness  $R_a$  of  $0.5 \mu\text{m}$ . The loss in wear pin mass was recorded and the reported density of the respective PEEK materials was used to calculate volumetric wear. Wear testing followed a full factorial experimental plan with factors including normal load, polymer molecular weight, and wear path. For the wear tests using paths a, c, and d, a total of four pins of each material were tested in randomized order to account for statistical variation. A follow up test was conducted with eight replications for the circular reciprocation (c) and variable velocity circular (b) paths at a contact pressure of 5.1 MPa. This was done in order to further investigate the effects of overlap of the wear path under the same velocity profile as reciprocation.

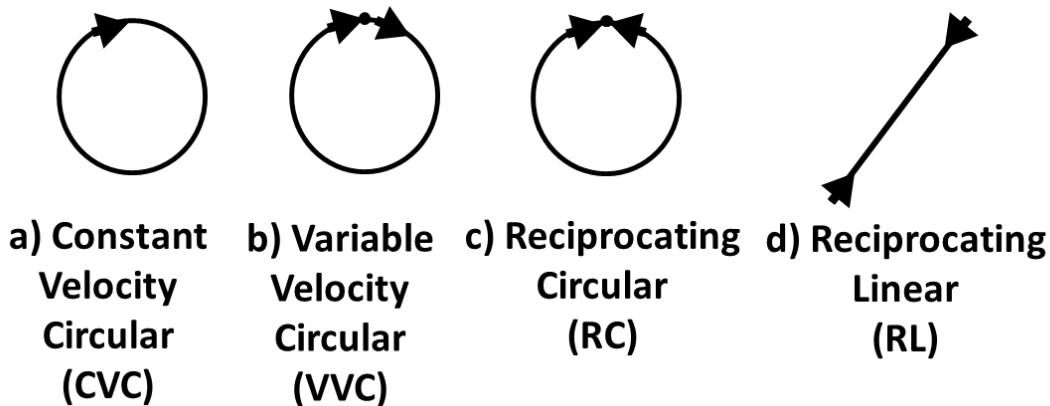


**Figure 1.** Wear path configurations used during the 2km sliding experiments. The CVC condition a) moved at a continuous velocity 200 mm/s for the first experiment. The paths in b,c,d accelerated at  $3 \text{ m/s}^2$  after stop to achieve 200 mm/s average velocity.

### 2.3 Transfer Film Measurement

It is commonly reported that in order for a transfer film to protect against wear it should be continuous and cover a majority of the surface. In this work, a quantifiable comparison was made between the films formed during variable velocity circular (VVC) and reciprocating circular (RC) motions. Using Image-J software, pictures of films were converted to 8-bit images and the light threshold was set between 165 and

250 as shown in Figure 2. The light threshold was adjusted to make only the film visible in the foreground. The film area was calculated and compared with a hypothetical area of total film coverage. For a 6.35mm pin moving in a 20mm diameter circle, a film that covers 100% of the surface should have an area of 398.9 mm<sup>2</sup>.

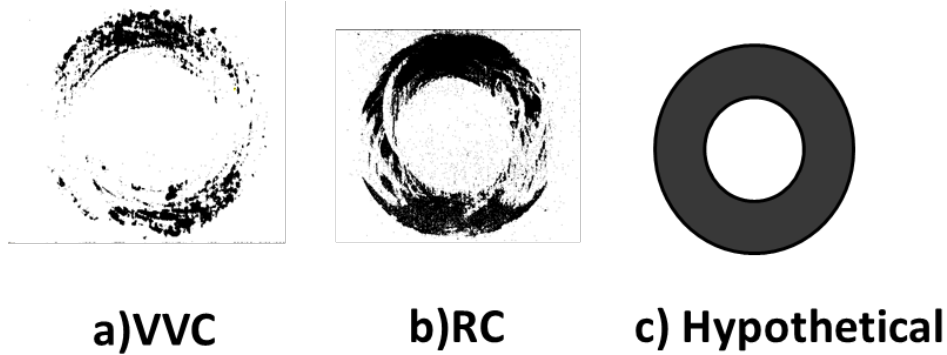


**Figure 2.** Area coverage measurement of transfer films using Image-J software.

Transfer films were also characterized using the distribution of film heights measured with a white light interferometry (WLI) based profilometer (Zygo). A three dimensional data map was produced, shown in Figure 3.a, and exported as a data file. Measurements were taken along the wear path at locations where sliding was perpendicular to the surface roughness orientation of the counterface, as shown in Figure 3.b. This was done to compare films formed under the same surface roughness conditions. In order to get a representative measurement of the entire transfer film at a particular sliding direction, eight measurements zones were analyzed. Therefore, the film height distribution represents a 0.7mm by 4mm area of transfer film. Data analysis was performed in Matlab in order to characterize the distribution of surface heights. It can be seen in Figure 3.c that there are two modes, which both closely follow a Gaussian distribution. In order to quantify the mean and standard deviation of the discrete data, a maximum likelihood estimation (MLE) was used to calculate a probability density function (PDF) for the distribution. The mathematical representation for the estimated PDF is shown in equation (1).

$$f(x; p, \mu_1, \mu_2, \sigma_1, \sigma_2) = (p) \frac{1}{\sigma_1 \sqrt{2\pi}} e^{-\frac{(x-\mu_1)^2}{2\sigma_1^2}} + (1-p) \frac{1}{\sigma_2 \sqrt{2\pi}} e^{-\frac{(x-\mu_2)^2}{2\sigma_2^2}} \quad (1)$$

The PDF is produced under the assumption that the data represents a mixture of two normal PDFs, represented by each exponential term in (1). The function is dependent upon the percent mixture of each normal PDF ( $p$ ) as well as the respective means ( $\mu$ ) and standard deviations ( $\sigma$ ). When given starting points for the mean, standard deviation, and percent mixture of the two PDFs, a built in Matlab function performs iterations until it converges at a solution for the function  $f(x)$ . The solution for the PDF parameters can then be used to characterize the relative film height and standard deviation. As shown in Figure 3.c, the leftmost mode reflects the ground surface roughness of the steel counterface and the rightmost mode indicates the height distribution of the transfer film. The white light interferometer quantifies height by identifying birefringence peaks as it vertically scans (40 $\mu$ m) the focal plane. During data processing, the heights are centered about zero and the relative distance between the plate mean ( $\mu_1$ ) and film mean ( $\mu_2$ ) are used to measure the film height. Negative and positive values of height, as shown in the figure, indicate the difference from the zero reference calculated with the maximum likelihood algorithm.

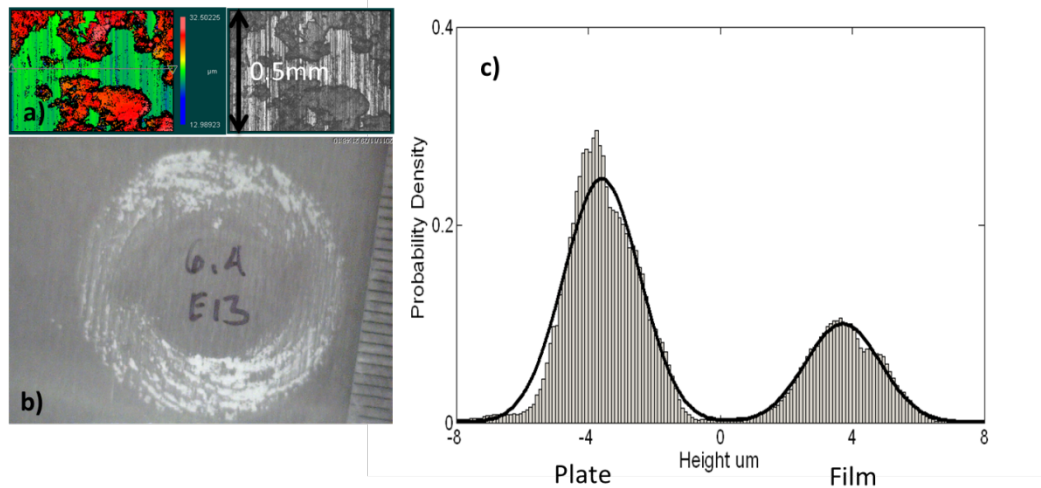


**Figure 3.** Transfer film characterization method using profilometer data.

#### 2.4 Wear Surface and Transfer Film Imaging

Images of both wear samples and counterfaces were taken in a JEOL-6400 scanning electron microscope (SEM), and were prepared using a light sputter-coating of gold-palladium. Sections of wear pins were cut with a diamond saw, and then imaged in secondary mode with an accelerating voltage of 15keV. In order to fit the counterfaces in the SEM, samples were cut using an electron discharge machine (EDM) and were washed in acetone prior to coating. The transfer films were imaged with an accelerating voltage of 15keV. Images were taken at location representing sliding perpendicular to surface roughness. The primary objective of this work was to understand how transfer film is deposited when sliding changes direction. Although there may be some contribution from differences in crystallinity or molecular weight to transfer film deposition, the transfer film study was limited to just one grade and contact pressure. Therefore, only the high molecular weight samples ('H') exposed to variable velocity circular (VVC) and reciprocating circular (RC) motions were examined in the SEM.

### 3. Results

#### 3.1 Wear

The results from all four wear test motion profiles of the two PEEK grades are plotted in Figure 4 for the calculated contact pressures of 1.1 and 5.1 MPa respectively. It should be noted that the sample sizes for (RC) and (VVC) at 5.1 MPa differ from the other groups. A follow up experiment was performed at these conditions to provide better statistical accuracy and therefore sample sizes are (n=12) and (n=8) respectively. Interestingly, despite the differences in molecular weight and contact pressure, the same general trends exist between the different wear paths. In the experiment, the sliding velocity and distance were kept constant so any differences seen in volumetric wear are attributed to the differences in motion. In all cases, the lowest wear resulted from reciprocating linear motion (RL), but the degree of difference depends on the molecular weight and pressure conditions. Tukey post-hoc analysis was performed on the wear data grouped by molecular weight and pressure as shown in Figure 4. In the plots, bars that are connected by roman numerals cannot be said to differ significantly with 95% confidence. At the 1.1 MPa pressure setting, the wear path has no effect on the high molecular weight sample, but is significant for all low molecular weight paths. However, with increasing pressure both samples differ significantly with respect to reciprocating motion. This is again most pronounced in the low molecular weight samples where all groups that differ do so with 99.9% confidence ( $p < 0.001$ ). Although the high molecular weight wear data does not appear to depend entirely on reciprocating, it should be pointed out that the (VVC) and (RC) paths were tested with a higher sample size and are less influenced by error. The Tukey test between

these two groups says they are significantly different ( $p < 0.001$ ) and therefore indicates that an explanation for why a reciprocating path produces the lowest wear is needed.

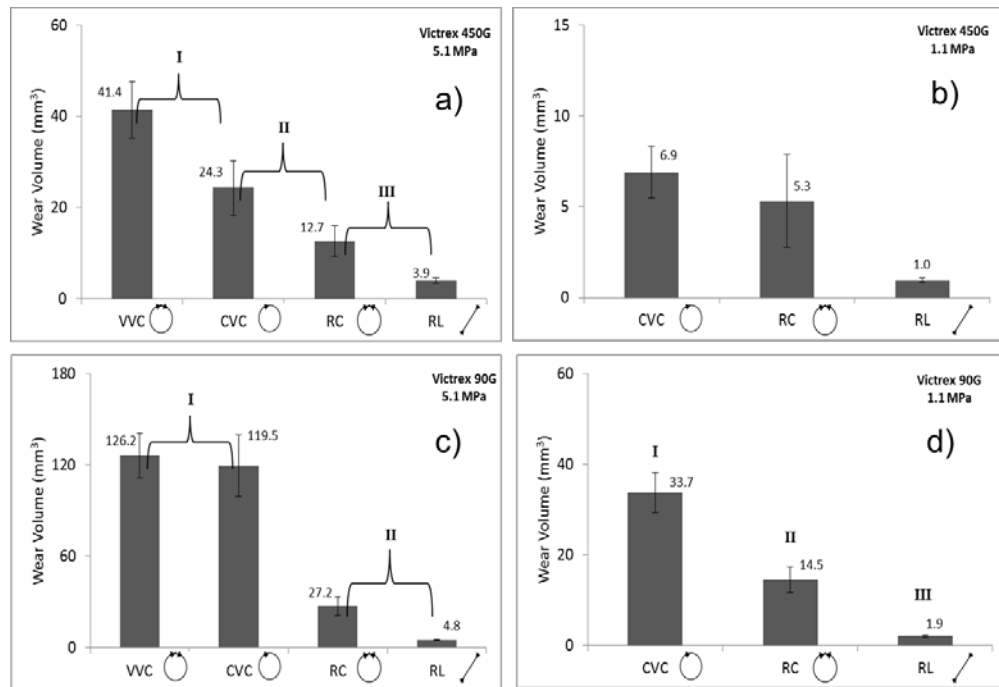


**Figure 4.** Wear volume data for all combinations of pressure, molecular weight, and path. Groups not connected by brackets are significantly different ( $p = 0.05$ ). Sample size ( $n = 4$ ) with the exception of VVC and RC in a), c).

### 3.2 Transfer films

Visually, it is apparent that a qualitative difference exists between films produced with reciprocating circular path (RC) and those that result from an overlapping (VVC) path as seen in Figure 5. Also, both circular wear paths (VVC) and (CVC) produce similar films despite different velocity profiles. It is reasoned that the film formation is dependent on whether the wear path reciprocates or overlaps and only the (VVC) condition was analyzed. Figure 5 shows the resulting films from high molecular weight samples tested at both low and high contact pressures and with the (VVC) and reciprocating (RC) wear paths. Comparing the films, two main differences exist. First, when contact pressure increases, the amount of material deposited on the counterface appears to increase as well. This effect is most prominent in the reciprocating films Figure 5.b and d. Secondly, films produced with the overlapping (VVC) wear condition appear qualitatively lumpier and more discontinuous even at low contact pressure. In particular, the reciprocating film in Figure 5.d has a smooth uniform appearance. It is also important to note that the same qualitative trends were seen in films produced with the low molecular weight samples. The calculated area coverage for high molecular weight samples under contact high pressures (5.1 MPa) confirms that there is a quantifiable difference between the wear paths as well. The mean coverage from the overlapping (VVC) and reciprocating (RC) tests are 19% and 40%, respectively.

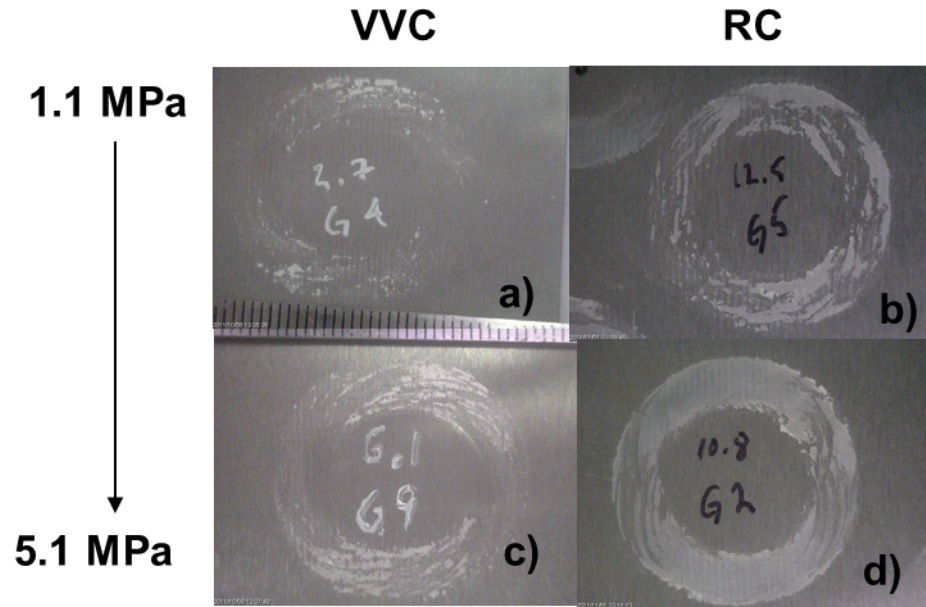


**Figure 5.** Transfer film images for VVC and RC sliding conditions at high and low pressure setting.

Similarly, analysis of the film height data from the same tests shows that reciprocating films are both thinner and have a more uniform distribution of heights. The probability density functions for the (VVC) and reciprocating (RC) conditions, shown in Figure 6, give quantitative differences between the film heights. A mean value for the film height with respect to the asperity heights can be represented by the difference between the PDF plate and film heights  $\mu_2 - \mu_1$ . Data from the eight (VVC) wear tests indicate that on average the film has a height of  $6.65\mu\text{m}$  and a standard deviation of  $1.52\mu\text{m}$ . The data from the reciprocating circular (RC) paths however are nearly half this with a film height of  $3.15\mu\text{m}$  and a standard deviation of  $0.53\mu\text{m}$ . It should also be noted that the measured standard deviation for the plate asperity heights are nearly identical for both data sets ( $\sim 1\mu\text{m}$ ).

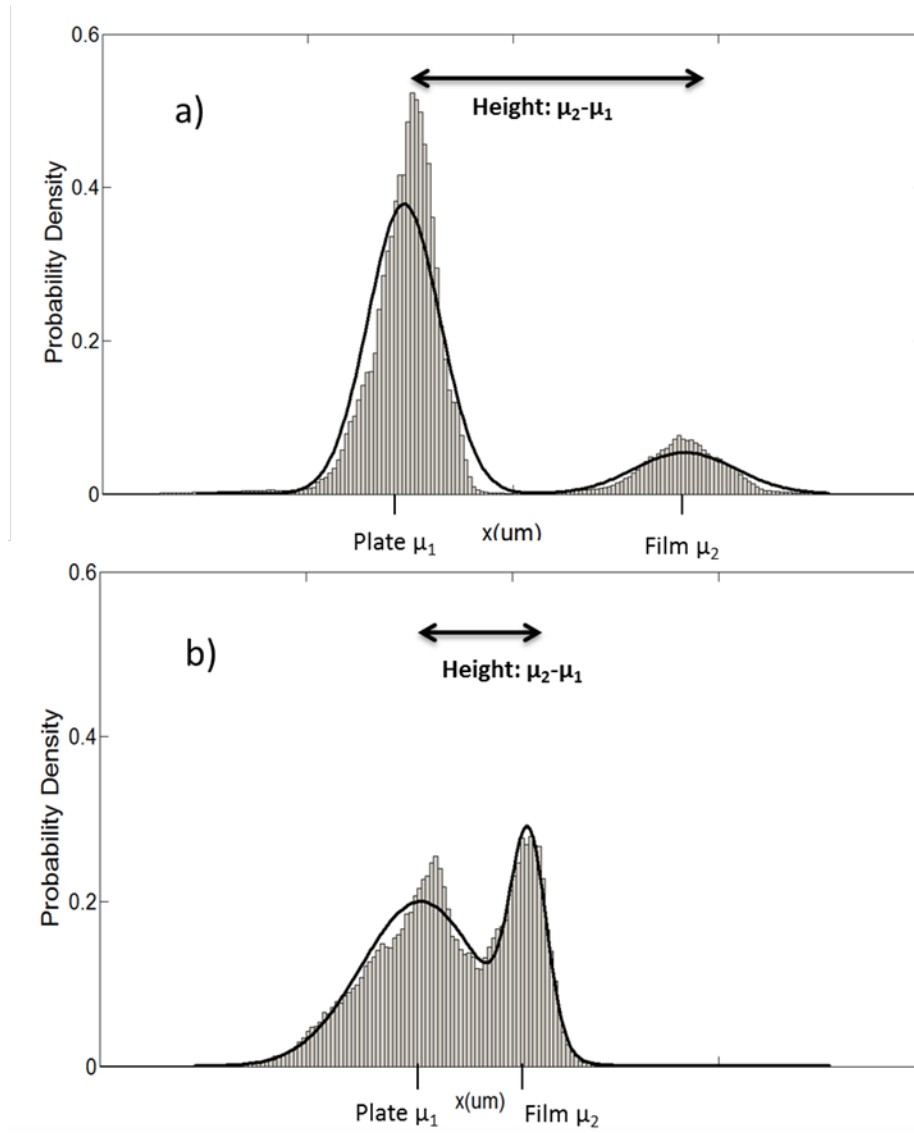


**Figure 6.** Transfer film height distributions. a) Film produced by (VVC) motion with height  $6.5\mu\text{m}$ . b) Film produced by (RC) motion with height  $3\mu\text{m}$ . X-axis tick marks on the top of the each figure are separated by  $5\mu\text{m}$ .

#### 4. Discussion

It is generally assumed that the presence of a transfer film during polymer wear protects the bulk material from the harder asperities. However, it is not fully understood what types of films are able to reduce wear and under what conditions these films form. During this study, it was found that quantifiably different films form as a result of changes in sliding direction for PEEK polymers. With all parameters fixed lower wear results from reciprocated sliding. When the sliding motion overlaps in a circular configuration, a lumpy discontinuous film is deposited. However, changing direction results in thinner, more uniform and more continuous transfer films. The rationale for why these differing films form can be explained by observation of film deposition on asperities. The scanning electron microscope (SEM) images of wear tracks on select counterfaces are shown in Figure 7.

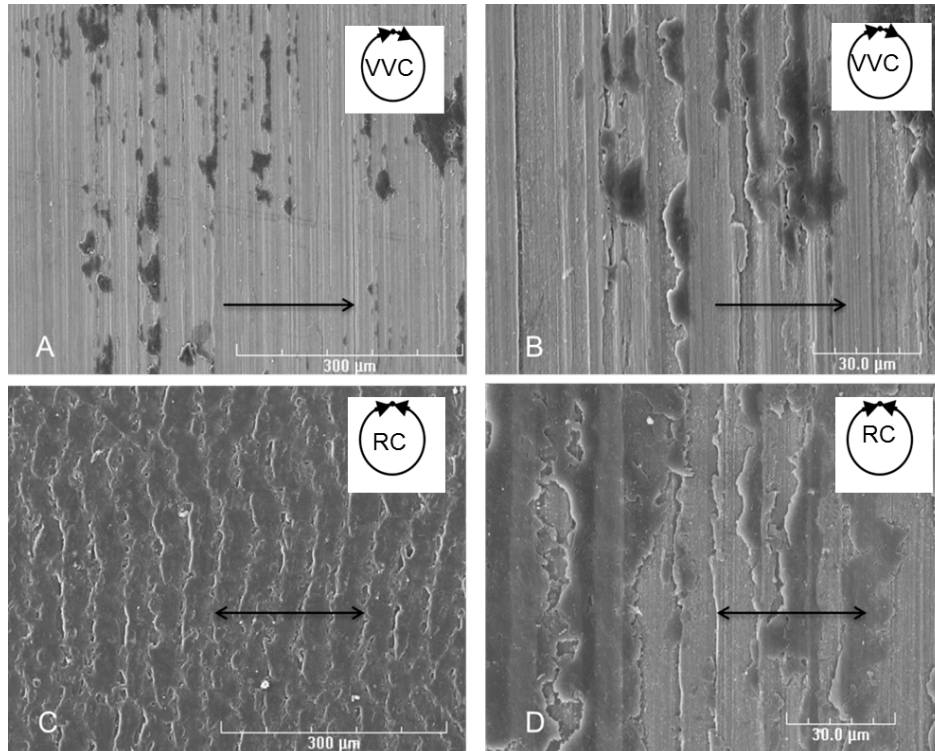


**Figure 7.** Scanning electron microscope (SEM) images of PEEK transfer films deposited on hardened D2 steel counterfaces. Arrows indicate the direction of sliding relative to the surface roughness. All samples were tested at 5.1 MPa nominal contact pressure with velocity profile indicated in the inset.

Material tends to deposit on one side of asperities in overlap sliding as shown in Figure 7.a and b. As the pin traverses the counterface, it can be surmised that the leading edge of the asperity penetrates the bulk polymer and removed material collects on the front flanks. The trailing edge of the asperity is left exposed because it is unable to make contact with the bulk. However, this does not explain why material does not deposit on the front of every asperity and why some material deposits over the top of multiple asperities. In order to understand this, we need to consider the distribution of asperity heights and space between asperities. Although plates were all ground to a surface roughness ( $R_a$ ) of  $0.5\mu\text{m}$ , the asperity height and spacing follows a Gaussian distribution. Within this range of heights, there is likely some critical height and spacing that deposited material cannot bridge. When an asperity of sufficient size is encountered, the removed material will pile up and agglomerate into large islands as shown in Figure 8. One large island has formed with a boundary clearly marked by the front edge of an asperity.

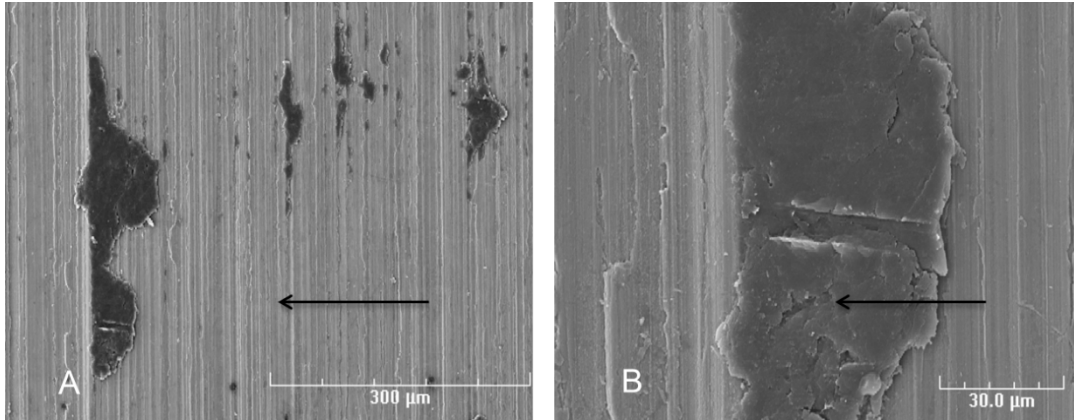


**Figure 8.** Scanning electron microscope (SEM) images of PEEK film trapped on the leading edge of an asperity. A) several large islands aligned with the asperities. B) 1000x image of the island in the lower left corner of A).

Theoretically, there is a height and spacing for asperities where every ridge can be filled by debris. In Figure 9.a, the asperities are evenly spaced and of the same height. As the pin moves over the counterface, each asperity penetrates into the bulk and plastically deforms the surface. Since the pin is able to contact all points, each leading edge will become covered with the entrapped debris. However, the trailing edge of asperities will remain exposed and will still be capable of abrading the pin. If the pin motion changes direction, the opposing edges can then be covered. The corollary to Figure 9.a is a counterface with ridges of varying heights and spacing. When the counterface is made up of tall peaks, shown in Figure 9.b, the pin surface is unable to contact each asperity. If the asperity is of sufficient height, it will plastically deform the pin surface such that it does not make contact with subsequent asperities. Wear debris collects on the face of these taller peaks, but a continuous transfer film does not form. Similarly, large spaces between ridges will prevent material deposition on every asperity shown in Figure 9.c. Although the pin can be worn by all peaks, the space between the ridges is too large to entrap debris.

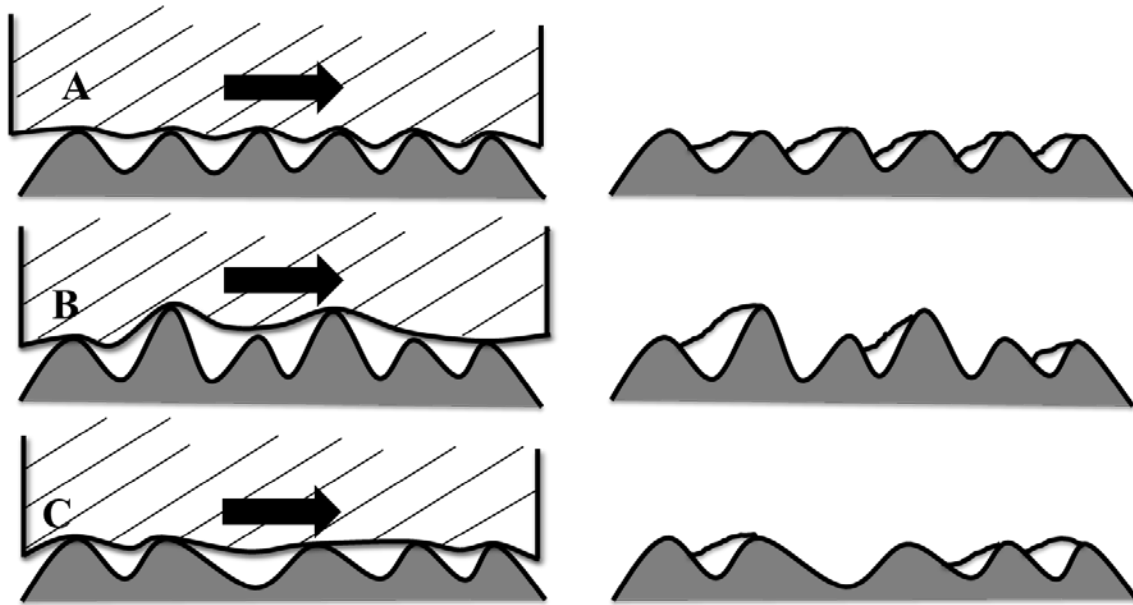


**Figure 9.** A theoretical illustration of how asperity height and spacing will influence material deposition during sliding. A) Uniform distribution of heights and spacing. B) Influence of tall asperity peaks. C) Influence of large gaps between asperities.

The distribution of asperity heights and spacing does not explain why a thin continuous film forms with a reciprocating wear path and why lower wear results. To understand this, we need to understand the wear mechanisms involved. Abrasive wear refers to material removal that is the result of a softer material rubbing against a hard rough surface. This appears to be the dominant mechanism for the wear path that overlaps with each pass as seen in Figure 10.c and d. The worn pin surface is scored and large craters develop from debris being continuously removed from the bulk. It is believed that a transfer film can protect against abrasive wear because the film's modulus more closely matches that of the polymer surface. As worn debris is deposited on the edges of asperities, fewer and fewer hard asperities make contact with the pin. At some point, the pin surface begins to contact the already deposited material and pull it over the top of each ridge. When the wear path reciprocates across both sides of asperities, a film can be drawn out as a continuous sheet over all asperities. This drawing out process manifests itself on the pin surface seen in Figure 10.a and b. With the exception of stuck debris, the reciprocating wear surface has a smooth topography absent of the scratches and craters seen during abrasive wear. Additionally, fibrous sheets appear to emanate from the surface of the pin. It is unclear whether these features originate from the bulk polymer or are drawn out from already deposited material. However, the drastic difference seen in the pin surface indicates a transition away from abrasive wear associated with the different wear path configuration.

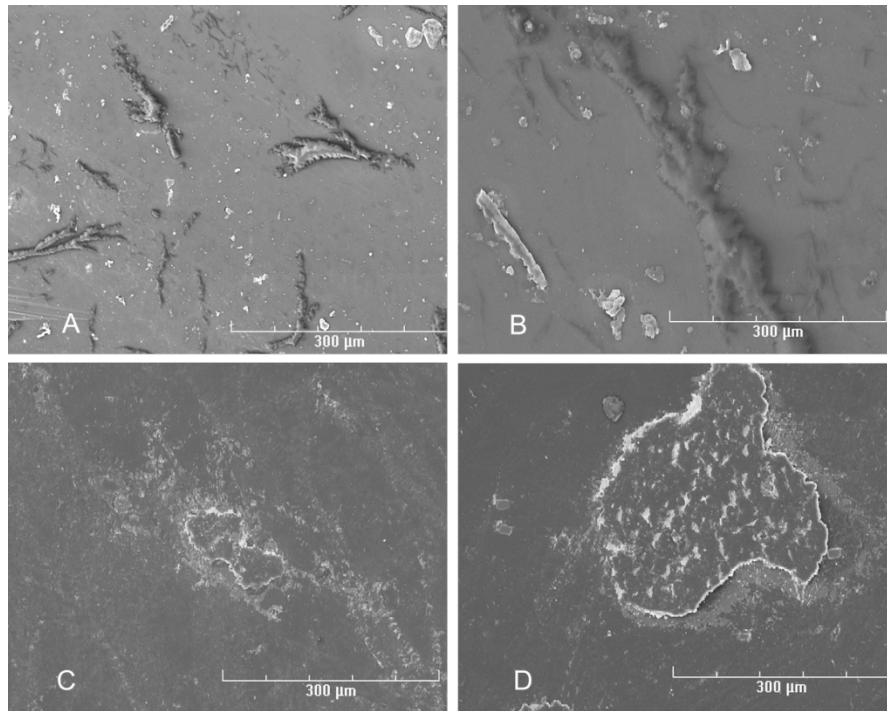


**Figure 10.** Scanning electron microscope (SEM) images of the worn PEEK pins after 2km sliding wear test for two different motion paths. A),B) Circular reciprocating motion. C),D) Circular overlap motion.

## 5. Conclusions

The following conclusions were drawn based on the results of this study:

1. When all other parameters are kept fixed, there is a statistically significant difference in the wear behavior of PEEK depending on the motion profile. At a contact pressure of 5.1 MPa, reciprocating motion results in lower wear with  $p < 0.001$ .
2. A quantifiable difference is observed in the PEEK transfer films deposited for circular wear paths depending on whether or not the motion changes direction with each pass. Films formed as a result of a circular overlapping path are observed to be lumpy and discontinuous relative to those of a circular reciprocating path. These differences are measurable in terms of the film's percent coverage and distribution of heights.
3. Lower wear is associated with a reciprocating wear path as a result of a transfer film that is able to cover hard rough asperities. Scanning electron microscope (SEM) inspection of the counterfaces shows that debris tends to collect on one side of an asperity for motion that overlaps in a single direction. If the pin is able to reciprocate, the trailing edge of asperities can be covered and prevented from making contact with the bulk.

## 6. Acknowledgements

The authors would like to thank the members of the consortium for Advancing Performance Polymers for Energy Applications (APPEAL) for providing the financial support and PEEK materials used in this study.

## 7. References

1. Wang, A., V.K. Polineni, A. Essner, M. Sokol, D.C. Sun, C. Stark, and J.H. Dumbleton, *The Significance of Nonlinear Motion in the Wear Screening of Orthopaedic Implant Materials*. Journal of Testing and Evaluation, 1997. **25**(2): p. 239-245.
2. Bragdon, C.R., D.O. O'Connor, J.D. Lowenstein, M. Jasty, and W.D. Syniuta, *The importance of multidirectional motion on the wear of polyethylene*. Proceedings of the Institution of Mechanical Engineers, Part H: Journal of Engineering in Medicine, 1996. **210**(3): p. 157-165.
3. Charnley, J., *WEAR OF PLASTICS MATERIALS IN THE HIP-JOINT*. Plastics and rubber, 1976. **1**(2): p. 59-63.
4. Charnley, J., *Low Friction Arthroplasty of the Hip*, 1979, Springer: New York.
5. Wang, A., D.C. Sun, S.S. Yau, B. Edwards, M. Sokol, A. Essner, V.K. Polineni, C. Stark, and J.H. Dumbleton, *Orientation softening in the deformation and wear of ultra-high molecular weight polyethylene*. Wear, 1997. **203-204**(0): p. 230-241.
6. Muratoglu, O.K., C.R. Bragdon, D.O. O'Connor, M. Jasty, W.H. Harris, R. Gul, and F. McGarry, *Unified wear model for highly crosslinked ultra-high molecular weight polyethylenes (UHMWPE)*. Biomaterials, 1999. **20**(16): p. 1463-1470.
7. Wang, A., C. Stark, and J.H. Dumbleton, *Mechanistic and morphological origins of ultra-high molecular weight polyethylene wear debris in total joint replacement prostheses*. Proceedings of the Institution of Mechanical Engineers, Part H: Journal of Engineering in Medicine, 1996. **210**(3): p. 141-155.
8. Sambasivan, S., D.A. Fischer, M.C. Shen, and S.M. Hsu, *Molecular orientation of ultrahigh molecular weight polyethylene induced by various sliding motions*. Journal of Biomedical Materials Research - Part B Applied Biomaterials, 2004. **70**(2): p. 278-285.
9. Lee, R.K., L.A. Korduba, and A. Wang, *An improved theoretical model of orientation softening and cross-shear wear of ultra high molecular weight polyethylene*. Wear, 2011. **271**(9-10): p. 2230-2233.
10. Pooley, C.M. and D. Tabor, *Friction and Molecular Structure: The Behaviour of Some Thermoplastics*. Proceedings of the Royal Society of London. Series A, Mathematical and Physical Sciences, 1972. **329**(1578): p. 251-274.
11. Biswas, S.K. and K. Vijayan, *Friction and wear of PTFE -- a review*. Wear, 1992. **158**(1-2): p. 193-211.
12. Lancaster, J.K., *Transfer Lubrication for High Temperatures: A Review*. Journal of Tribology, 1985. **107**(4): p. 437-443.
13. Ovaert, T.C. and H.S. Cheng, *Counterface topographical effects on the wear of polyetheretherketone and a polyetheretherketone-carbon fiber composite*. Wear, 1991. **150**(1-2): p. 275-287.
14. Briscoe, B., *Wear of polymers: an essay on fundamental aspects*. Tribology International, 1981. **14**(4): p. 231-243.
15. Stachowiak, G.W. and A.W. Batchelor, *Engineering tribology*2005: Elsevier Butterworth-Heinemann.
16. Friedrich, K., J. Karger-Kocsis, and Z. Lu, *Effects of steel counterface roughness and temperature on the friction and wear of PE(E)K composites under dry sliding conditions*. Wear, 1991. **148**(2): p. 235-247.
17. Ramachandra, S. and T.C. Ovaert, *The effect of controlled surface topographical features on the unlubricated transfer and wear of PEEK*. Wear, 1997. **206**(1-2): p. 94-99.